



HAL
open science

Electronic Structure and Excited States of the Collision Reaction $O(3P) + C_2H_4$: A multiconfigurational Perspective

Francesco Talotta, Sabine Morisset, Nathalie Rougeau, David Lauvergnat,
Federica Agostini

► **To cite this version:**

Francesco Talotta, Sabine Morisset, Nathalie Rougeau, David Lauvergnat, Federica Agostini. Electronic Structure and Excited States of the Collision Reaction $O(3P) + C_2H_4$: A multiconfigurational Perspective. *Journal of Physical Chemistry A*, 2021, 125 (28), pp.6075-6088. 10.1021/acs.jpca.1c02923 . hal-03365881

HAL Id: hal-03365881

<https://cnrs.hal.science/hal-03365881>

Submitted on 5 Oct 2021

HAL is a multi-disciplinary open access archive for the deposit and dissemination of scientific research documents, whether they are published or not. The documents may come from teaching and research institutions in France or abroad, or from public or private research centers.

L'archive ouverte pluridisciplinaire **HAL**, est destinée au dépôt et à la diffusion de documents scientifiques de niveau recherche, publiés ou non, émanant des établissements d'enseignement et de recherche français ou étrangers, des laboratoires publics ou privés.

Electronic Structure and Excited States of the Collision Reaction $O(^3P)+C_2H_4$: A Multiconfigurational Perspective

Francesco Talotta,^{*,†,¶} Sabine Morisset,[‡] Nathalie Rougeau,[‡] David Lauvergnat,[†]
and Federica Agostini^{*,†}

[†]*Université Paris-Saclay, CNRS, Institut de Chimie Physique UMR8000, 91405, Orsay,
France*

[‡]*Université Paris-Saclay, CNRS, Institut des Sciences Moléculaires d'Orsay, UMR8214,
91405, Orsay, France*

[¶]*Université Paris-Saclay, CNRS, Institut des Sciences Moléculaires d'Orsay, UMR8214,
91405, Orsay, France*

E-mail: francesco.talotta@universite-paris-saclay.fr; federica.agostini@universite-paris-saclay.fr

Abstract

We present a study of the $O(^3P)+C_2H_4$ scattering reaction, a process that takes place in the interstellar medium and is of relevance in atmospheric chemistry as well. A comprehensive investigation of the electronic properties of the system has been carried out based on multiconfigurational ab-initio CASSCF/CASPT2 calculations, using a robust and consistent active space that can deliver accurate potential energy surfaces in the key regions visited by the system. The paper discloses detailed description of the primary reaction pathways and the relevant singlet and triplet excited states at the CASSCF and CASPT2 level, including an accurate description of the critical configurations, such as minima and transition states. The chosen active space and the

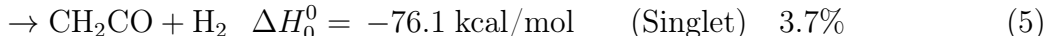
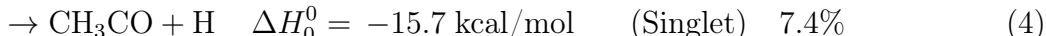
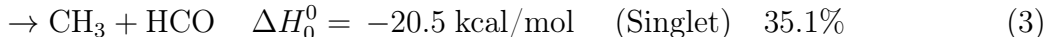
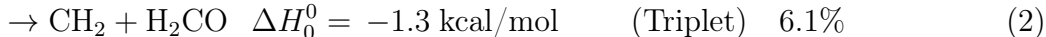
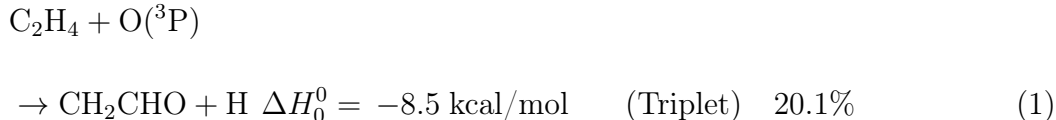
CASSCF/CASPT2 computational protocol are assessed against coupled-cluster calculations, to further check the stability and reliability of the entire multiconfigurational procedure.

1 Introduction

The reaction between ethylene C_2H_4 and triplet oxygen $O(^3P)$ is a chemical process that gained interest in the field of atmospheric chemistry and astrochemistry,^{1,2} due to its relevance in specific chemical problems such as the degradation of the space ships traveling on low Earth orbits.³⁻⁷ Furthermore, this reaction can be considered as a prototype for both experimental and theoretical studies in the field of chemical reaction dynamics, because of the rather small number of atoms involved, as well as the occurrence of radiationless relaxation phenomena involving electronic states of different spin multiplicity. Accordingly, this system and the related products have been widely studied especially in the last fifteen years.^{3,8-18} In particular, crossed molecular beams experiments and quantum-classical trajectory surface hopping calculations showed that the reaction develops on both singlet and triplet potential energy surfaces (PESs) via an intersystem crossing (ISC) process.^{15,16} These studies have assessed the branching ratios between the various product channels and estimated both angular and translation distributions of the products at different collision energies.

In Ref. [15], surface-hopping simulations have been performed on the lowest singlet (S_0) and triplet (T_1) PESs, coupled by a spatially constant spin-orbit coupling (SOC). The PESs have been fitted and shifted according to ab-initio single point energies obtained from different methods, such as complete active space self-consistent field (CASSCF), multi-reference configuration interaction (MRCI) and coupled-cluster with single-double and perturbative triple (RCCSD(T)) calculations. It was shown that among the many exothermic product

pathways, the following are the most probable to occur:¹⁵



where the exothermicity values at 0 K are taken from previous coupled-cluster calculations.¹⁵

For each reaction channel we indicate the corresponding surface-hopping probability for a collision energy of 0.36 eV, as reported in Ref. [19]. On account of these results a reaction mechanism has been proposed and is summarized in Figure 1 (and Figure S18 of the Supporting Information). Note that the numerical values of the energies reported in the figures refer to this work, whereas in the discussed below we refer to the values reported in Ref. [15]. The differences between our results and Ref. [15] are summarized in Figure 1, and will be amply described in the course of paper.

The chemical process begins with a collision between the oxygen atom O(³P) and the ethylene molecule C₂H₄ on the lowest triplet PES T₁, to form a triplet biradical ³CH₂CH₂O. In order to reach this configuration, the system has to overcome a small barrier of about 0.13 eV, related to the transition state TS1. The reaction then develops on either triplet or singlet PESs. In particular, pathways (1) and (2) should stay on the triplet T₁ (see Figure 1, upper panel): the biradical can dissociate into the products H + CH₂CHO via the transition state TS3 with a barrier height of about 1.00 eV, or dissociate into the products CH₂ + H₂CO by breaking the C-C bond via TS4, facing a barrier of about 1.15 eV. The final parts

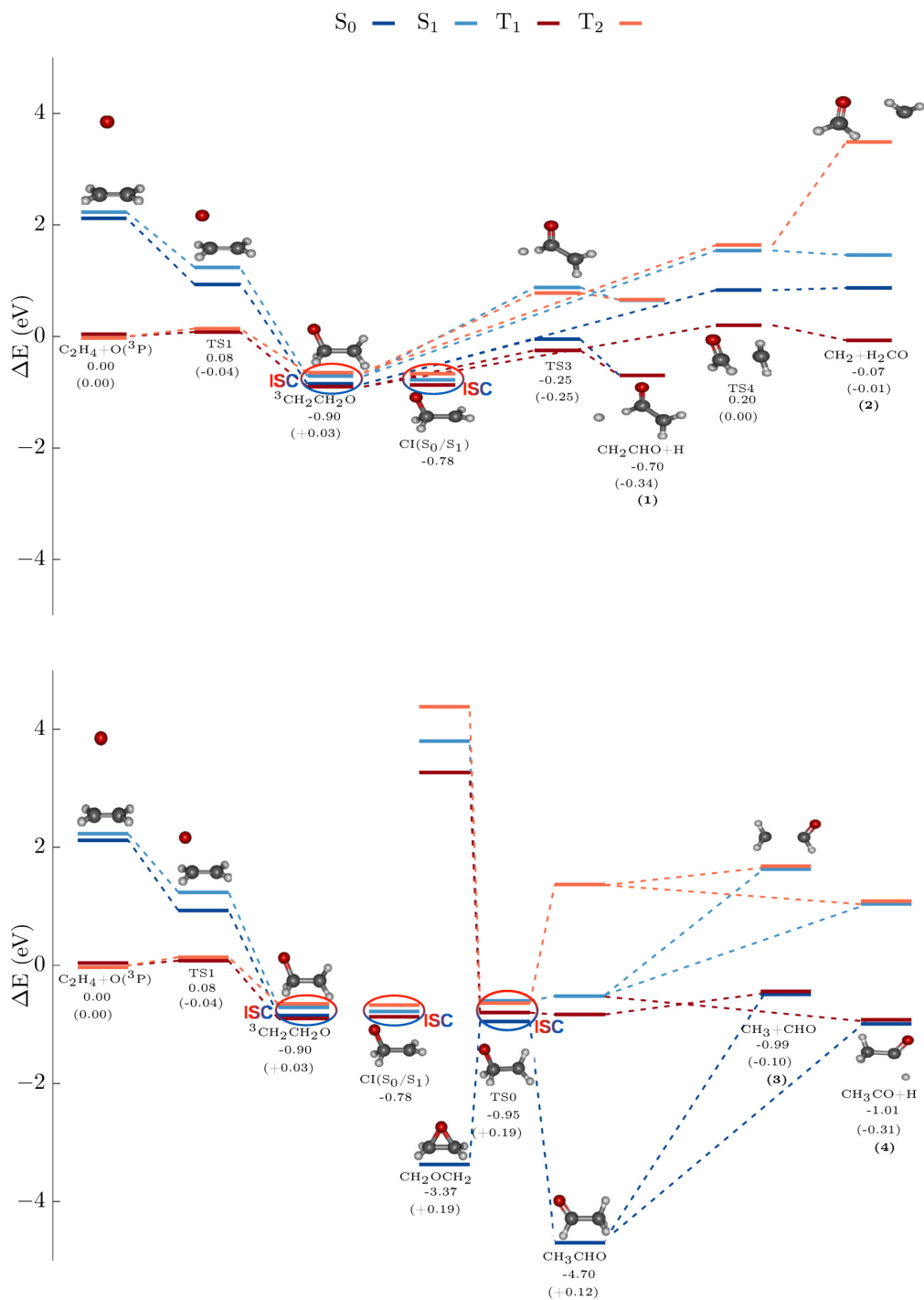


Figure 1: Summary and schematic representation of the critical regions of the singlet and triplet PES from MS2-CASPT2 calculations. In the upper panel we report the results for pathways (1) and (2) terminating in the triplet, whereas in the lower panel we report the results for pathways (3) and (4) terminating in the singlet. Relative energies (in eV) are computed with respect to the collision geometry $O(^3P) + C_2H_4$. The values in parentheses report the differences with respect to the values of Ref. [15]. Circled regions indicated as ISC highlight the configurations where intersystem crossing is expected to occur.

of pathways (3) to (5) should develop on the lowest singlet PES (S_0) through ISC from the triplet T_1 ¹⁵ (see Figure 1, lower panel, where we show pathways (3) and (4)). This triplet to singlet spin-flipping occurs in a particular region of PESs centered around the biradical ${}^3\text{CH}_2\text{CH}_2\text{O}$, where S_0 and T_1 are almost degenerate and coupled by a small SOC of $\sim 35 \text{ cm}^{-1}$ (which is not surprising due to the nature of the atomic species involved). The singlet biradical denoted as TS0 on the S_0 PES comes from the ISC and lies about 0.14 eV lower than the triplet counterpart. It can undergo a 1,2-H shift and isomerize to the singlet CH_3CHO or form the oxirane CH_2OCH_2 by oxygen migration and ring-closure. The oxirane will eventually isomerize to CH_3CHO and further dissociate into various products of pathways (3), (4), and (5) on the singlet PES S_0 , such as $\text{CH}_3 + \text{HCO}$, $\text{H} + \text{CH}_3\text{CO}$, or $\text{CH}_2\text{CO} + \text{H}_2$.

Both theory and experiments agree with this mechanistic picture, even though some differences between the quantum-classical simulations and crossed molecular beams experiments still exist. For instance, cross section and branching ratio values differ for some particular reactive pathways, such as the $\text{CH}_2\text{CHO} + \text{H}$ or the $\text{CH}_2 + \text{H}_2\text{CO}$.¹⁶ As a matter of fact, it should be noted that previous quantum-classical dynamics calculations have been systematically performed on S_0 and T_1 fitted PESs with a constant value of SOC, and the PESs have been rescaled according to CASSCF, CCSD(T) and MRCI single point energies. As will be discussed in the course of the paper, and as shown in Figure 1, a conical intersection between the two lowest singlet states appears at a geometry where SOC is important, and is energetically accessible. Therefore, the role of the excited states might play a role in the reaction dynamics, allowing the system to undergo internal conversion (IC), i.e. population transfer between states of the same spin multiplicity, along with ISC. Nonetheless, effects due to excited states have usually been neglected,^{3,15} which allowed, together with the use of fitted PESs,¹⁵ to propagate a large number of trajectories, and to achieve, consequently, good statistics for the prediction of cross sections and branching ratios. Significant contributions to the characterization of the electronic structure of this system have been made

based on density functional theory (DFT) methods.^{3,12,18,20-22} However, DFT is unable to describe systems that show a significant multiconfigurational character, especially when the system undergoes bond breaking or bond formation, which is exactly the situation studied here. DFT simply has problems in handling fragmentation which, instead, multiconfigurational methods can properly account for. Therefore, the CASSCF and the complete active space second-order perturbation theory (CASPT2) are suitable methods of choice to study the electronic structure of this scattering reaction. It is important to add that the presence of the conical intersection between S_0 and S_1 prevents one to use the linear-response time-dependent DFT (LR-TDDFT) approach as well, which is not able to capture such a degeneracy.^{18,20}

The purpose of the present work is to accurately investigate the electronic structure properties along the reactive pathways listed above, employing a consistent and reliable CASSCF/CASPT2 computational procedure. The study has been carried out assuming a static perspective, provided by the computation of the potential energy landscapes of relevant electronic states along the reaction paths, including the description of the relevant singlet and triplet excited states and the related SOC. The first two singlet and triplet states (S_0 , S_1 , T_1 , T_2) have been taken into account, since those states are very close in energy near the biradical region. We successfully identified an active space that changes smoothly along several reaction paths. This active space shows neither discontinuities in the PESs nor sudden changes of the electronic properties.

The work reported in this paper is significant for various reasons. First, it provides solid and suitable basis for potential ab-initio on-the-fly dynamics calculations (not restricted to surface-hopping approach) especially regarding the choice of the active space, whose orbitals could also serve as starting point for studies on similar systems.²³⁻²⁶ In addition, such a small molecular system, $O + C_2H_4$, seems to manifest interplay between ISC and IC, mediated by SOC and by the S_0 - S_1 conical intersection, respectively. This feature makes it an excellent candidate to be a test-case for new excited-state molecular dynamics methods, very much in

the spirit of the recently proposed molecular Tully models.²⁷ Therefore, we make available to the community, in the most transparent way, in the paper and in the Supporting Information: active-space orbitals, geometries and electronic characters of the identified critical configurations, geometries and energies along the internal reaction coordinates (IRCs) and linear interpolated transit paths (LITP) in internal coordinates used to study the potential energy profiles. Finally, our work illustrates the limitation of the CASSCF approach – so far, the only accessible approach to on-the-fly simulations for this system – for instance in terms of the energetics. In particular, we will point out a systematic overestimation of CASSCF energies with respect to the CASPT2 results, which will need to be taken care of for on-the-fly dynamics.

The paper is organized as follows. In Section 2 we provide details about the computational methods used to carry out this study. In Section 3.1 we discuss the electronic and the nondynamical correlation properties of the most important geometries involved in the pathways (1) to (5). In particular, referring to Figure 1, we analyze the singlet minima CH_2OCH_2 (oxirane) and CH_3CHO (acetaldehyde), which are transient configurations ultimately leading to the products of pathways (3), (4) and (5), along with the singlet transition state TS0 and the S_0 - S_1 conical intersection. On the lowest triplet PES, as shown in Figure 1, we identify and analyze the triplet transition state TS1 leading to the formation of the triplet biradical $^3\text{CH}_2\text{CH}_2\text{O}$, as well as the triplet transition states TS3 and TS4, yielding the products (1) and (2), respectively. In Section 3.2 we discuss the various scattering pathways by means of IRC and LITP calculations. The singlet pathways (3) to (5) become accessible via the 1,2-H shift isomerization mentioned above, which involves the transition state TS0; starting with oxirane and acetaldehyde the final products are formed without involving additional transition states. The $\text{O}(^3\text{P}) + \text{C}_2\text{H}_4$ entrance pathway along the triplet PES involves passing via the transition state TS1. The triplet pathways towards the formation of the products of (1) and (2) involve the transition states TS3 and TS4. Our conclusions are reported in Section 4.

2 Methods

Multiconfigurational ab-initio calculations were performed using the CASSCF and CASPT2 methods.²⁸ These calculations have two main objectives: (i) to determine the electronic structure and multiconfigurational properties of the system, (ii) to characterize singlet and triplet potential energy surfaces, related to the reactive pathways (1) to (5). All reference CASSCF single-point and geometry optimization calculations have been performed distributing 12 electrons in 12 orbitals. This active space (denoted CAS(12,12)) is shown in Figure 2 for oxirane, and was chosen in view of the reactive scattering process, which mainly involves the O and C atoms, with C-C and C-O bond breaking and bond formation. The active space orbitals include thus the pairs of σ/σ^* , and π/π^* for C-C, the 2s and the three 2p oxygen orbitals, and the π orbital for the C-H. The pair of virtual orbitals $3p_x$ and $3s$ were also included to stabilize the active space and to recover some dynamic correlation. This active space is thus suited to describe all the relevant excited states involved in the scattering reaction, which involve $\pi \rightarrow \pi^*$ or $n \rightarrow \pi^*$ transitions (vide infra).

The active space has been carefully checked after every single point calculation, to ensure the stability and reliability of the CASSCF wavefunction. Our analysis points out that the active space shown in Figure 2 is sufficient to describe the reaction channels (1) to (4) along with their energetics. In particular, as illustrated in Figure S1 of the Supporting Information, inclusion of the orbital $3p_x$ is essential to capture the C-H bond breaking underlying pathways (1), (3) and (4) above. The same active space, however, rotates along pathway (5) and, while the energy profiles look smooth, we cannot conclude on the reliability of this active space to describe correctly pathway (5). Therefore, we will not describe in detail this low-probability reaction pathway. This is because the results presented in this work shall be intended as a preliminary study for dynamics on-the-fly simulations. With this idea in mind, we opt towards identifying a stable and smoothly-varying active space that is able to capture the majority of the reaction channels of the title reaction (about 70% according to the probabilities (1) to (4)), rather than adapting the active space to the various reaction

channels, which would prevent from a straightforward application in on-the-fly dynamics.

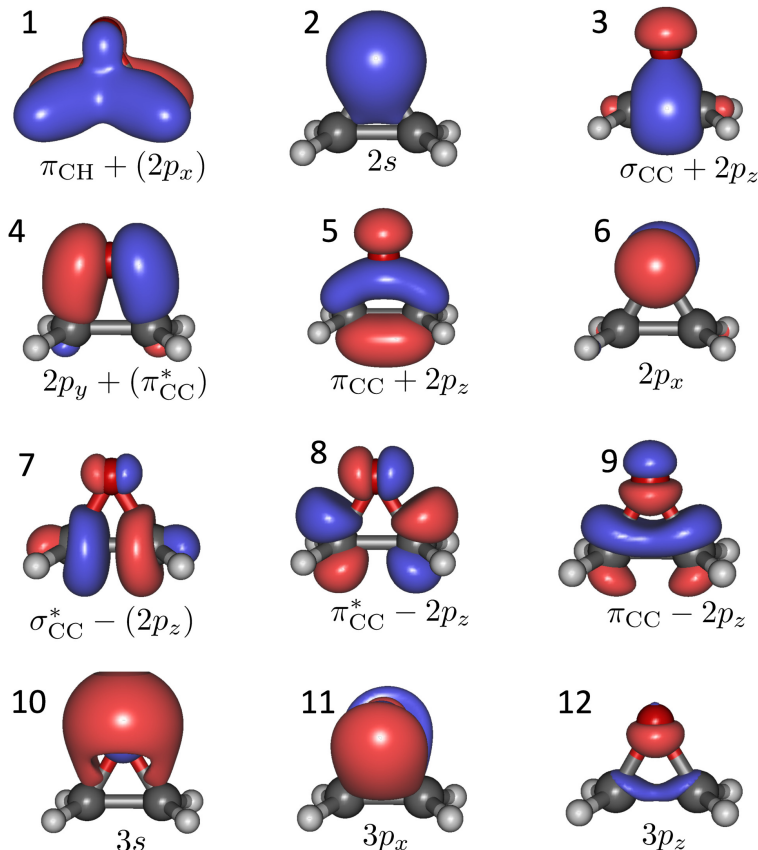


Figure 2: Active space represented in terms of natural orbitals and obtained from the SA2-CASSCF(12,12)/ANO-L-VTZP calculation at the CH_2OCH_2 geometry (isovalue: 0.08). Orbitals in round bracket mean a marginal contribution to the active orbital. The names are assigned by identifying the ethylene contribution and by adding the oxygen orbitals; the name of orbital 12 is taken from Ref. [12].

State-averaged calculations over two states were performed separately for singlet and triplet states (denoted SA2-CASSCF(12,12)). This number of states stabilizes the active space, providing at the same time the description of all the relevant states, as only the lowest two singlet and triplet states are energetically accessible for this scattering process. Multi-state CASPT2 (MS-CASPT2) calculations were then performed using a standard IPEA shift¹ of 0.25 au^{29,30} and a level shift of 0.3 au was carefully chosen in order to avoid intruder states. Separate MS-CASPT2 calculations have been performed for each singlet and triplet multiplicity, on the lowest two states (denoted MS2-CASPT2) for both multiplicities. In

¹IPEA stands for: IP=ionization potential, EA=electron affinity.

all calculations, the Douglas-Kroll-Hell Hamiltonian and the Cholesky decomposition with a threshold of 10^{-6} au were used along with the ANO-L-VTZ all-electron basis for O³¹ and C and ANO-L-VDZ for the H atoms.³² Some tests with a larger basis set did not show any notable change in the energies. For this reason we decided to proceed with the ANO-L-VTZ and ANO-L-VDZ basis sets as they are a good compromise between accuracy and computational cost. All the CASSCF and CASPT2 calculations were performed with OpenMolcas package.³³ The biradical index y of the molecules was investigated according to the natural orbital occupation number (NOON) analysis, i.e. on the basis of the occupation number (n) of the LUMO-like orbital resulting from the CASSCF calculation. The LUMO-like orbital has been identified by looking at the CASSCF wavefunction configurations, detecting for each state the unoccupied natural orbital towards which the excitation has been carried out. The biradical index ranges from 0% to 100% (for a pure biradical state).^{34,35} All geometry optimizations have been performed at the CASSCF level, as CASPT2 optimizations using a CAS(12,12) active space was not possible with our computational resources. Indeed, although CASPT2 singlet point energy calculations are relatively fast and similar to a CASSCF single point calculation in terms of computational cost, calculations of energy gradients and derivative couplings, which are necessary for non-adiabatic dynamics, are prohibitive with CASPT2. To the best of our knowledge, as of today, there are no quantum chemistry codes able to compute singlet and triplet gradients and derivative couplings efficiently through resolution of analytical equations, which would be the only efficient strategy to follow for the dynamics. SOC calculations were performed at selected critical configurations within the spin-orbit state interaction frame³⁶ using the singlet and triplet spin-free CASSCF wavefunctions as basis for the spin-orbit Hamiltonian. Dynamic electron correlation effects were included by using the MS-CASPT2 as the diagonal elements of the spin-orbit Hamiltonian.

Additional single point calculations on the optimized CASSCF geometries using the coupled-cluster with single, double and perturbative triple excitation CCSD(T)^{37,38} method were performed with the ORCA 4.1.2^{39,40} computational package, to give further support to

the MS-CASPT2 results. For such calculations, the aug-cc-pVTZ basis set⁴¹ has been used for all atoms.

3 Results and discussion

In Section 3.1, we determine stationary points and transition states on the lowest singlet and triplet PESs, and we discuss in detail their electronic properties, devoting some attention to the multiconfigurational character of the electronic wavefunctions. In Section 3.2, we analyze the relevant reaction paths either using an IRC analysis when transition states can be identified along the lowest singlet and triplet PESs or using a LITP analysis on the lowest singlet PES in the absence of transition states.

Since this system has been studied in previous work,¹⁴⁻¹⁶ we present our findings in comparison with those studies. In particular, unless explicitly indicated, the reference results are those of Ref. [15].

3.1 Electronic structure and multiconfigurational properties

The first two singlet and triplet states (S_0 , S_1 , T_1 , T_2) were computed for all the minima and transition states involved in pathways (1) to (5) at the SA2-CASSCF and MS2-CASPT2 levels of theory. Cartesian coordinates for each optimized geometry can be found as Supporting Information. Table 1 and Table 2 show the vertical transition energies calculated considering S_0 as reference, and details about the character of the main electronic configuration for the singlet and triplet optimized geometries, respectively. The tables also show the weight of the leading configuration (C^2) as a square of the CI coefficients C , retrieved from the analysis of the CASSCF wavefunction.

In all cases, the CASPT2 excitation energies are in very good agreement with previous theoretical calculations^{12,15} and experiments,^{42,43} with the maximum error usually below 0.2 eV. The CASSCF values are, however, systematically overestimated by maximum 0.4 eV.

We attribute this inconsistency to the lack of dynamic electron correlation in the CASSCF wavefunction. The energy difference between CASSCF and CASPT2 tends to be more significant in some particular cases, such as for the singlet minima CH_2OCH_2 and CH_3CHO , where the dynamic correlation effects are stronger as both molecules are the only species for which all electrons form Lewis pairs. Nevertheless, the accuracy of the CASPT2 energies for all the optimized species guarantees that the CASSCF/CASPT2 computational procedure and the chosen active space are accurate enough to describe the electronic structure of the system in the relevant regions visited along the reaction.

The geometries discussed below are identified either on S_0 or on T_1 . For each geometry we will analyze the electronic properties of all states S_0 , S_1 , T_1 , T_2 .

3.1.1 Singlet minima, transition state and conical intersection

The analysis of the electronic properties has been performed for the critical configurations optimized on the S_0 PES, identified along the reaction path via TS0 , namely $\text{CH}_2\text{OCH}_2 \rightarrow \text{TS0} \rightarrow \text{CH}_3\text{CHO}$. A summary of the observations reported below can be found in Table 1. The four geometries identified in the table can be found in Figure 1.

- (a) For the CH_2OCH_2 (oxirane) molecule, whereof we show the CAS(12,12) active space in Figure 2, the MS-CASPT2 first singlet excited state S_1 is predicted at 7.18 eV, in good agreement with previous TD-DFT results¹² and close to the experimental value of 7.24 eV.⁴² This state is obtained by a transition from the oxygen lone pair orbital $2p_x$ to the virtual orbital $3p_z$ (1B_1 transition): this result is in disagreement with the earlier TD-DFT calculations (using different functionals) at the same geometry¹² which predict a contribution from a s -like virtual orbital; however, this same result is in agreement with more recent cDFT calculations.⁴⁴ The triplet states T_1 and T_2 are placed by the MS-CASPT2 at 6.65 eV and 7.76 eV respectively, namely 0.53 eV below and 0.58 eV above the singlet S_1 , respectively. The T_1 state is described by transitions involving the same orbitals of the S_1 state (3B_1 transition), whereas the T_2 state is described

Table 1: Summary table of the singlet optimized species discussed in the text. The electronic states considered in our calculations are listed in the first column, along with the corresponding SA2-CASSCF (second column) and MS2-CASPT2 (third column) transition energies (eV) taking the energy of S_0 as reference. When available, experimental values are provided as well (forth column). The character of the main configuration and its weight are shown in the fifth and sixth columns, respectively. Note that the generic names π and π^* refer to the CC bond and are not defined via Figure 2 since they do not belong to the oxirane configuration.

state	CASSCF ΔE	CASPT2 ΔE	expt.	character	C^2
CH ₂ OCH ₂					
S ₀	0.000	0.000		<i>closed-shell</i>	0.93
S ₁	7.440	7.176	7.239 ⁴²	$2p_x \rightarrow 3p_z$	0.93
T ₁	6.949	6.649		$2p_x \rightarrow 3p_z$	0.94
T ₂	7.942	7.758		$\pi_{CC} + 2p_z \rightarrow 3p_z$	0.94
CH ₃ CHO					
S ₀	0.000	0.000		<i>closed-shell</i>	0.91
S ₁	4.499	4.202	4.280 ⁴³	$2p_x \rightarrow \pi^*$	0.92
T ₁	4.168	3.887	3.970 ⁴³	$2p_x \rightarrow \pi^*$	0.95
T ₂	6.189	6.094	5.990 ⁴³	$\pi \rightarrow \pi^*$	0.96
TS0					
S ₀	0.000	0.000		<i>closed-shell</i>	0.33
				$2p_x \rightarrow \pi^*$	0.33
S ₁	0.316	0.351	-	$2p_y \rightarrow \pi^*$	0.69
T ₁	0.093	0.144	-	$2p_x \rightarrow \pi^*$	0.93
T ₂	0.265	0.312	-	$2p_y \rightarrow \pi^*$	0.94
CI (S ₀ -S ₁)					
S ₀	0.000	0.000		<i>closed-shell</i>	0.39
S ₁	0.000	0.003	-	$2p_y \rightarrow \pi^*$	0.79
T ₁	-0.102	-0.090	-	$2p_x \rightarrow \pi^*$	0.93
T ₂	0.092	0.108	-	$2p_y \rightarrow \pi^*$	0.94

by a transition from the $\pi_{CC} + 2p_z$ orbital to the virtual orbital $3p_x$ (3A_1 transition). According to CASPT2, at this geometry the three excited states S₁, T₁, T₂ result to be too high in energy to be involved in the O(³P) + C₂H₄ reaction mechanism. For instance, in an astrochemistry context, the energy scales at play are much lower than 6-7 eV, thus preventing the system to reach S₁, T₁ or T₂ at this geometry. The analysis of the CASSCF wavefunction shows that the weight of the most important configuration (C^2) for all four states is larger than 0.90, indicating a single-reference character of

the electronic structure at this geometry. The biradical index y is 0% according to the NOON analysis, in agreement with the closed-shell nature of the main electronic configuration.

(b) For the CH₃CHO (acetaldehyde) molecule, the S₁ state is generated by a $2p_x \rightarrow \pi^*$ transition ($^1A''$) and is placed by the MS-CASPT2 at 4.20 eV, very close to the experimental value of 4.28 eV.⁴³ The triplet states T₁ and T₂ are placed respectively at 3.89 eV and 6.10 eV, again in good agreement with the experimental values of 3.97 eV and 6.00 eV.⁴³ As in the oxirane molecule, the T₁ state shares the same kind of excitation as the S₁ state ($^3A''$), whereas T₂ shows a $\pi \rightarrow \pi^*$ excitation ($^3A'$). The character and energetic order of the three states is in agreement with what was previously reported in the literature for this molecule.⁴³ The analysis of the CASSCF wavefunction shows similar results to the oxirane, with the C^2 values larger than 0.90, meaning a single-reference character for all the electronic states at this geometry. The biradical index is 0% in this case as well.

(c) Regarding the singlet transition state, denoted TS0, CASPT2 predicts the first singlet excited state S₁ 0.35 eV higher than S₀, whereas the triplet states T₁ and T₂ are predicted at 0.14 eV and at 0.31 eV, respectively. Hence, in this region the electronic states are much closer in energy if compared to the other two species, in agreement with previous electronic structure calculations at the same geometry.¹⁵ It is worth noting that in this case the S₁ and T₂ states are obtained by a different excitation. Indeed, the active orbital π_z smoothly rotates towards the second oxygen lone pair orbital $2p_y$ during the oxirane C-O bond breaking, (see Figure S2 of the Supporting Information) resulting in two $2p_y \rightarrow \pi^*$ states. The weights of the leading configuration of the CASSCF wavefunction C^2 are less than 0.90 for the two singlet states, indicating a strong static electron correlation. In particular, for the S₀ state, there are two leading configurations (*closed-shell* and $2p_x \rightarrow \pi^*$) contributing with an equal weight of 0.33.

Another, less important, configuration $2p_x \rightarrow \pi^*$ with a weight of 0.18 derives from the coupling with the nearby S_1 state. A closer look at the electron density and CASSCF configurations revealed the coexistence of two resonance structures, that have been already described in some early work about the excited state oxirane ring-opening reaction,^{45,46} i.e. a biradical and a zwitterion configuration, both contributing to the final CASSCF wavefunction for the S_0 state. The biradical form corresponds to the $2p_x \rightarrow \pi^*$ and the $2p_y \rightarrow \pi^*$ configurations, whereas the zwitterion corresponds to the *closed-shell* configuration. This bifunctional character, related to spin localization and pairing, is consistent with the value of the biradical index $y = 62\%$. The S_1 state displays also a strong multiconfigurational character with a value of C^2 of 0.69 for the leading configuration, due to the coupling with the lower state S_0 . This last observation suggests the presence of a nearby conical intersection between the two states. Regarding the triplet states, in this case the value of the weight C^2 is higher than 0.90, revealing a single-reference character for both states. The biradical character is confirmed by the value $y = 100\%$ of the biradical index for both, and the spin density analysis, which shows one electron localized on the π^* carbon atom and the other localized on the $2p_x$ orbital for the T_1 state, and on $2p_y$ for the T_2 state (see Figure S3 of the Supporting Information). According to previous surface-hopping calculations,¹⁵ after the scattering event, the reaction proceeds towards this biradical transition zone, where ISC from the triplet to the singlet PES is expected to occur. The close proximity of those states, together with a non-negligible SOC, creates appropriate conditions for singlet to triplet ISC. Further CASPT2 calculation estimates a SOC value between 20 and 40 cm^{-1} , in agreement with the mean value of 35 cm^{-1} used in Ref. [15]. In particular, the two pair of states S_0 - T_1 and S_1 - T_2 show the same value of 20 cm^{-1} , whereas the pair of states S_0 - T_2 and S_1 - T_1 show a value of 40 cm^{-1} . This difference is compatible with the El-Sayed⁴⁷ rule, in the sense that S_0 and T_1 share the same electronic character in their electronic transitions, and the same for S_1 and T_2 .

The particular electronic properties of this transition-state region have been reported in several theoretical studies on the same system reaction.^{12,15,21,44} According to the basic quantum multielectron theory, a singlet biradicaloid needs two determinants to be correctly represented whereas a triplet biradicaloid needs only one determinant.⁴⁸ Thus, in every structure where the biradicaloid character becomes important the singlet states systematically show a strong multireference character whereas the triplets retain a singlet reference character.

- (d) The last singlet configuration that has been optimized is the S_0 - S_1 conical intersection. The optimized geometry is qualitatively very similar to the one found by Tapavicza et al. [12] with a C_s symmetry, and differs from the TS0 geometry by a CH_2 rotation. It is worth noting that the S_0 - S_1 degeneracy is maintained at CASPT2 level, with an energy gap between S_0 and S_1 of only 0.003 eV. Interestingly, the electronic properties are very similar to TS0, with a superposition of biradical and zwitterion character for the S_0 state, and a pure biradical character for the S_1 and the two triplet states. At this geometry, the triplet states are very close to the two degenerate singlet states, with T_1 lying only 0.09 eV below S_0 - S_1 , and T_2 lying 0.11 eV above. SOC calculations show very similar results to TS0, with values ranging between 20 and 40 cm^{-1} , making this geometry a good candidate for the occurrence of ISC, due to the close proximity of the singlet and triplet states and the non-negligible SOC. Note that, this geometry is energetically accessible during the scattering reaction, since the electronic-state manifold is placed by both CASSCF and CASPT2 at almost the same energy as TS0, as shown in Figure 1 and Figure S18 of the Supporting Information. Accordingly, in the region near the conical intersection, IC and ISC might occur as competing effects, and the slightly different geometries of the S_0 - S_1 conical intersection and of TS0 might affect the reactivity in different ways.

Table 2: Summary table of the triplet optimized species discussed in the text. The electronic states considered in our calculations are listed in the first column, along with the corresponding SA2-CASSCF (second column) and MS2-CASPT2 (third column) transition energies (eV) taking the energy of S_0 as reference. The character of the main configuration and its weight are shown in the fourth and fifth columns, respectively. Note that the generic names π and π^* refer to the CC bond and are not defined via Figure 2 since they do not belong to the oxirane configuration. In TS3 and TS4 the orbitals acquire an “atom-like” character, thus we refer here to $2p_C$ and $1s_H$.

state	CASSCF ΔE	CASPT2 ΔE	character	C^2
${}^3\text{CH}_2\text{CH}_2\text{O}$				
S_0	0.000	0.000	$2p_x \rightarrow \pi^*$	0.55
S_1	0.123	0.144	$2p_x \rightarrow \pi^*$	0.33
T_1	-0.091	-0.051	$2p_x \rightarrow \pi^*$	0.92
T_2	0.169	0.202	$2p_y \rightarrow \pi^*$	0.93
TS1				
S_0	0.000	0.000	<i>closed-shell</i>	0.72
S_1	0.465	0.309	$2p_x \rightarrow \pi^*$	0.82
T_1	-0.648	-0.849	$2p_x \rightarrow \pi^*$	0.90
T_2	-0.611	-0.788	$2p_y \rightarrow \pi^*$	0.90
TS3				
S_0	0.000	0.000	<i>closed-shell</i>	0.59
S_1	1.048	0.927	$2p_x + 2p_C - 1s_H \rightarrow 2p_x - 2p_C - 1s_H$	0.81
T_1	-0.292	-0.203	$2p_y \rightarrow \pi_{CC}$	0.90
T_2	0.895	0.828	$\pi_{CO} \rightarrow \pi_{CC}^*$	0.90
TS4				
S_0	0.000	0.000	<i>closed-shell</i>	0.49
S_1	0.843	0.709	$2p_x + \sigma_{CC} \rightarrow 2p_C$	0.63
T_1	-0.778	-0.638	$2p_x + \sigma_{CC} \rightarrow 2p_C$	0.88
T_2	0.888	0.803	$2p_x \rightarrow 2p_C$	0.88

3.1.2 Triplet minima and transition states

The analysis of the electronic properties has been performed for the minima and transition states configurations optimized on the T_1 PES. Those configurations have been identified along the reaction paths via TS1, namely $\text{O} + \text{C}_2\text{H}_2 \rightarrow \text{TS1} \rightarrow {}^3\text{CH}_2\text{CH}_2\text{O}$, via TS3, namely ${}^3\text{CH}_2\text{CH}_2\text{O} \rightarrow \text{TS3} \rightarrow \text{H} + \text{CH}_2\text{CHO}$, and via TS4, namely ${}^3\text{CH}_2\text{CH}_2\text{O} \rightarrow \text{TS4} \rightarrow \text{CH}_2 + \text{CHO}$. In general, the two triplet states T_1 and T_2 listed in Table 2 show a single-reference character with a C^2 value larger than 0.90, whereas the singlet states have a strong multiconfigurational character, due to the biradicaloid nature of the system in certain regions

of the PES. As for the singlet, the triplet critical configurations can be identified in Figure 1.

(e) The triplet minimum ${}^3\text{CH}_2\text{CH}_2\text{O}$ displays a molecular geometry very similar to the singlet transition state TS0. The two geometries are located very close on the PES, sharing therefore very similar electronic properties. CASPT2 calculations show the four electronic states energetically very close to each other. In particular, the energy gap between T_1 and S_0 is only 0.05 eV, whereas S_1 and T_2 are placed 0.15 eV and 0.20 eV higher than S_0 , respectively. All the states are described by transitions involving the same orbitals found in TS0. Furthermore, the energy difference between the TS0 S_0 and the ${}^3\text{CH}_2\text{CH}_2\text{O}$ T_1 is just 0.05 eV, meaning that the states are almost degenerate according to MS-CASPT2 calculations. This gap is lower than the value of 0.14 eV previously reported by Fu et al. [15] but still in fair good agreement. The multiconfigurational character results to be stronger than TS0 for the singlet states. A detailed examination of the CASSCF wavefunction reveals that S_0 and S_1 are strongly coupled to each other, sharing the same kind of excitations. Both states are formed by three leading determinants. For S_0 the most important among those determinants is the single excitation from the lone pair oxygen orbital $2p_x$ to the opposite carbon atom π^* orbital, which is surprising because such a transition couples two states that are localized on different moieties. Such configuration serves also as leading configuration for the S_1 state, although with a smaller weight of 0.33. The other two configurations of S_0 are the *closed-shell* and the transition from the second lone pair oxygen orbital $2p_y$ to the opposite carbon atom π^* orbital. Note that the *closed-shell* configuration contributes to the S_0 state with a weight of only 0.15, whereas for S_1 it shows a larger contribution of 0.25. SOC calculations at this geometry show the same values as for the TS0 transition state, i.e. 20 cm^{-1} for the pairs S_0 - T_1 and S_1 - T_2 , whereas 40 cm^{-1} for the pairs S_0 - T_2 and S_1 - T_1 . The analysis of the biradical index reveals a larger biradical character for the singlet states ($y = 76\%$ for S_0 and $y = 68\%$ for S_1) if compared to the TS0 state, whereas the triplet states are again pure biradicals with $y = 100\%$.

(f) The next geometry that has been studied is the transition state TS1, of utmost importance since it is the first transition state encountered by the system upon the scattering event.¹⁵ This configuration represents also a cut-off between the asymptotic region where the two reactants are well far apart from each other, and the region where the C-O σ bond is established. The multireference character of the singlet states is less important if compared to the previous geometry. The electronic states result to be energetically further away from each other. In particular, according to CASPT2, the S_1 state is 0.31 eV higher than S_0 , whereas T_1 and T_2 are placed 0.85 eV and 0.79 eV lower than S_0 . The analysis of the CASSCF wavefunction shows the *closed-shell* configuration contributing to the S_0 state with a weight coefficient C^2 of 0.72 and no other leading configuration contributing to the state. Similarly, the S_1 state shows only one important configuration represented by the excitation from the oxygen lone pair orbital $2p_x$ to the C-C π^* orbital. The triplet states are also formed by one leading determinant which contributes in both cases with a coefficient $C^2 = 0.90$. Both states are formed by the same kind of excitations already encountered in the triplet minimum studied above. Note that for each of the three states S_1 , T_1 , T_2 the leading determinants have the same character as the triplet minimum ${}^3\text{CH}_2\text{OCH}_2$ and TS0, meaning that no state changes occur from one geometry to another. For S_0 the biradical index is 30%, much smaller than the previous geometry whereas for the other states the biradical character is always close to $y = 100\%$. The small biradical index of S_0 is in agreement with the less significant multiconfigurational character of this state and with the fact that the system is in a configuration close to two separate reactants C_2H_4 and $\text{O}({}^3\text{P})$. SOC calculations show values in the range of 20 to 40 cm^{-1} , however, the larger energy gap between the singlet and triplet states makes this geometry a less favorable candidate for ISC, in agreement with the previous mechanistic picture,¹⁵ which predicts ISC near the singlet TS0 or the triplet ${}^3\text{CH}_2\text{OCH}_2$.

(g) The transition state TS3 is related to pathway (1) which involves the H-C bond disso-

ciation on the T_1 PES to form the products $H + CH_2CHO$. According to MS-CASPT2, at this transition state, the singlet states are close in energy to the triplet states. S_0 and T_1 are separated by 0.20 eV whereas S_1 and T_2 by 0.10 eV. Note, however, that the pair states S_0-T_1 and S_1-T_2 are quite far from each other by about 0.8 eV (see Table 2 and Figure 1 for reference). The analysis of the CASSCF wavefunction reveals that, similarly to the other studied species, the singlet states have a very strong multiconfigurational character: for S_0 the leading configuration has weight 0.59 and is *closed-shell* whereas for S_1 the weight of the leading configuration is 0.81. The triplet states reveal a single-references character, as both show 0.90 for the weight of the leading configuration. The biradical index is 57% for the S_0 state, meaning that for such state the multiconfigurational character is due to the combination of both bond dissociation and biradical character. For S_1 the biradical index is 95%, whereas the triplet states T_1 and T_2 are pure biradical states as the value of the biradical index is equal to 100%. The analysis of the Mulliken spin density for the triplet states reveals that part of the spin density is localized on the leaving hydrogen atom, suggesting a C-H homolytic bond breaking for such states. The character of the excited states result to be different with respect to the other transition states seen above, meaning that we are sampling a different portion of the PES. Indeed, the active molecular orbitals shown in Figure 2 smoothly rotate towards more “atomic-like”, localized orbitals, reflecting the partial dissociation of the molecule into two separated chemical systems. Nevertheless, the oxygen lone pair (either $2p_x$ or $2p_y$) continues to appear in the transitions for the three states S_1 , T_1 , and T_2 . For this last triplet state, the lone pair undergoes an in-phase mix with a carbon p orbital, forming a π_{O-C} bonding orbital. Although at this configuration the singlet and the triplet states are close in energy, SOC analysis reveals that the values are not large enough to promote ISC. Indeed, SOC values are not negligible for the pair of states S_0-T_2 and S_1-T_1 (around 35 cm^{-1}), however, they are too far apart for ISC.

(h) The transition state TS4 is related to the C-C dissociation channel (2) on the triplet T_1 . According to the MS-CASPT2, the singlet states S_0 and S_1 are well separated from each other (see Table 2), with S_1 0.71 eV higher than S_0 . The same happens for the triplet states, with the T_1 and T_2 states placed 0.64 eV lower and 0.80 eV higher than S_0 . As for the other transition states, the analysis of the CASSCF wavefunction reveals that the singlet states have a stronger multiconfigurational character than the triplet states. Notably, the S_0 state is the sum of three important determinants, with the *closed-shell* leading configuration contributing with a weight of 0.49. The other two configurations contribute to the state with a weight of 0.15, and one is also the leading configuration of the S_1 state, i.e. the excitation from the molecular $2p_x + \sigma_{CC}$ (oxygen lone pair combined with a bonding σ between the two carbon atoms) towards a carbon p atomic orbital, as indicated in Table 2. Such configuration contributes to S_1 with a weight of 0.63. The two triplet states show a much weaker multireference character, as the weight of the leading configuration is equal to 0.88, with no other important contributions from other configurations. The T_1 state has the same character as the S_1 state, whereas T_2 is the excitation from the oxygen lone pair $2p_y$ to the opposite carbon p orbital, suggesting a strong biradical character. Indeed, for S_1 , T_1 , T_2 , the orbitals involved in the electron configurations are the same orbitals shown in the spin density calculation (see Figure S3 of the Supporting Information). The analysis of the biradical index is consistent with these observations, as for S_0 the biradical character is $y = 50\%$, in agreement with the mixed character of the state formed by three important determinants. For S_1 the biradical index is 74% again in agreement with the configuration of the state, whereas for the triplet states $y = 100\%$. Regarding SOC, for this configuration the situation is similar to the TS3 transition state: the couplings are not negligible only between pair of states that are far away in energy, suggesting that ISC is not promoted in this case.

3.2 Potential energy profiles

Previous multiconfigurational studies reported in Refs. [14–16] focused on the lowest singlet and triplet PES for the entire scattering process. Participation of higher singlet and triplet states was mentioned then but not thoroughly investigated. The aim of the present MS-CASPT2 calculations is to shed light on the behavior of the excited states, using a multi-reference ab-initio method capable of describing both static and dynamic electron correlation in a balanced way for all the electronic states involved. We are going to analyze the CASPT2 energy profiles obtained from IRC calculations for the transition states TS0, TS1, TS3, TS4 shown in Figures 3, 4, 5, 6. The summary Figure 1 includes all pathways together (the corresponding figure based on CASSCF calculations is shown in Figure S18 of the Supporting Information). Along the last parts of pathways (3) and (4) transition states are not encountered, thus the analysis of the potential energy profiles is based on LITP, to reach the dissociation limit starting from the minimum of the lowest singlet PES. These results are reported in Figures 7 and 8. We will compare and assess such profiles against the corresponding CASSCF and CCSD(T) potential energy profiles, available in the Supporting Information in Figures S4 to S17. Energies in Hartree and eV are also available for the CASSCF and CASPT2 calculations in Tables S1 to S24 of the Supporting Information.

In general, the ground state CASPT2 profiles (either S_0 or T_1) are in very good agreement with the ones obtained by previous calculations¹⁵ as seen by the small differences in Figure 1. Energy gaps at the configurations identified in Sections 3.1.1 and 3.1.2 and in the asymptotic regions are well reproduced, with a maximum deviation always below 0.2 eV, except for the asymptotic region related to TS3 where the error is 0.38 eV. It is remarkable that, despite IRC optimizations were performed at CASSCF level, all the minima and transition states are reproduced by the MS2-CASPT2 single point calculations (see Figures S4, S5, S6 and S7 of the Supporting Information for the corresponding CASSCF energy profiles). This fact ensures that the CASSCF optimized structures are accurate enough, confirming the robustness of the active space shown in Figure 2, able to deliver accurate geometries in

several parts of the PES, despite the fact that CASSCF misses some dynamic correlation.

In the figures below, as well as in the corresponding figures in the Supporting Information, we report the potential energy profiles along IRCs and LITPs. Each IRC has been identified from the transition-state analysis, and the energy profiles have been organized considering negative values of the IRCs on the left and positive value on the right. For consistency among the figures, we impose the negative regions to be asymptotic configurations. LITPs are employed for the analysis of the last parts of reaction pathways (3) and (4) presented in the Introduction, since the lowest PESs do not present transition states. As mentioned in Section 2, pathway (5) is not analyzed in detail since the instability of the active space of Figure 2 prevents us from reporting a conclusive analysis.

- *1,2-H shift singlet isomerization channel.* Figure 3 presents the MS2-CASPT2 energy profiles for the lowest singlet and triplet states, related to the 1,2-H shift isomerization IRC between the oxirane CH_2OCH_2 and the acetaldehyde CH_3CHO . Acetaldehyde is a transient configuration which yields pathways (3) to (5) presented in the Introduction. The ground state PES S_0 is very well reproduced by the MS2-CASPT2 (as can be seen in Figure 3 showing the energy differences in brackets with Ref. [15]). The three excited states S_1 , T_1 , T_2 show a similar behavior in terms of potential energy profiles, different from S_0 . Starting from the oxirane geometry, when S_0 increases in energy, S_1 , T_1 and T_2 decrease in energy. As a result, the energy gap between S_0 and the excited-state manifold is considerably reduced near the transition state region TS0, where the four states become almost degenerate. In this region, SOC reaches its maximum value of 40 cm^{-1} , making ISC very likely to occur. The analysis of the CASSCF wavefunction reveals that in this region the system becomes highly multiconfigurational, acquiring a strong biradical character, as discussed in Section 3.1. Going from TS0 towards the acetaldehyde CH_3CHO minimum, the singlet ground state S_0 decreases in energy, and the excited states increase in energy, showing a maximum half-way between TS0 and CH_3CHO . The CASSCF potential energy profiles in Figure S4 of the Supporting In-

formation qualitatively agree with the topology of the corresponding CASPT2 curves, although relative energies are more accurate in the latter. The most noticeable difference between the CASSCF and CASPT2 energy profiles is the separation between the two minima: according to CASSCF the acetaldehyde is placed 1.76 eV lower than oxirane, whereas this value is reduced to 1.33 eV according to CASPT2. Nevertheless, both theories concur that the excited states play a role only near the transition state TS0, where ISC from the triplet to the singlet may occur, in line with the previous theoretical calculations.¹⁵

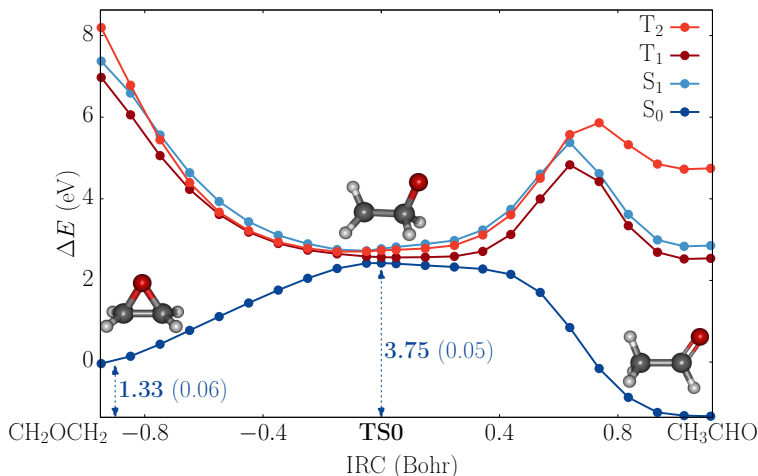


Figure 3: MS2-CASPT2 singlet and triplet potential energy profiles along the IRC pathway related to TS0, between the oxirane CH_2OCH_2 and the acetaldehyde CH_3CHO . Relative energies are in eV, and values in parentheses are the differences with respect to the values obtained in Ref. [15].

CCSD(T) calculations on the ground state S_0 and the triplet excited state T_1 in Figure S11 of the Supporting Information confirms the substantial multiconfigurational character at TS0. Compared to the MS2-CASPT2 results, relative energy deviations of less than 0.1 are obtained with CCSD(T) near the two minima. Larger errors are obtained in the region near TS0 for the singlet ground state S_0 only, in agreement with the strong nondynamical electron correlation gained by such state in this region. Figure S11 of the Supporting Information clearly shows that the proton transfer underlying this pathway develops via qualitatively different mechanisms along S_0 if the PES

is computed based either on CASSCF/CASPT2 or on CCSD(T): What is a transition state in CASSCF/CASPT2, i.e. TS0, becomes a minimum in CCSD(T). An incorrect interpretation of this isomerization pathway might be expected if the reaction were to develop via two transition states and an intermediate specie, i.e. CCSD(T), rather than via a single transition state, i.e. MS2-CASPT2. The T1 diagnostic vector for the S_0 state, which provides a useful indicator of the importance of nondynamical electron correlation effects,^{49,50} shows the lowest values right at the two minima CH_2OCH_2 and CH_3CHO , whereas much larger values > 0.02 are obtained at TS0. The evolution of the multiconfigurational character along the IRC can be appreciated in Figure S10 and in Figure S11 of the Supporting Information by looking at the T1 diagnostic curve, which acquires a gaussian-like shape peaked near TS0. Thus, according to this diagnostic criterion, significant nondynamical correlation effects are expected in the region near this geometry and single-references methods like CCSD(T) and DFT are potentially unreliable in describing electronic states of singlet spin multiplicity. Note also how the overall CCSD(T) T_1 topology is in good agreement with the CASPT2 profile, since such electronic state shows a single-references character (see Table 1).

- $O(^3P)+C_2H_4$ triplet entrance channel. Figure 4 presents the MS2-CASPT2 potential energy profiles for the two lowest triplet and singlet states along the IRC between the reactants $O(^3P)+C_2H_4$ and $^3\text{CH}_2\text{CH}_2\text{O}$, i.e. the minimum on the triplet PES, via the transition state TS1. The overall topology of the T_1 potential energy profile is again in good agreement with previous theoretical observations.¹⁵ Two minima and one transition state are located right at the reactants, $^3\text{CH}_2\text{CH}_2\text{O}$, and TS1, with the same energetic order: the triplet minimum $^3\text{CH}_2\text{CH}_2\text{O}$ is placed 0.90 eV lower than the asymptotic limit. The associated T_1 adiabatic energy barrier of 0.08 eV measured at TS1 is also in excellent agreement with the previous theoretical results which reported a value of 0.12 eV.

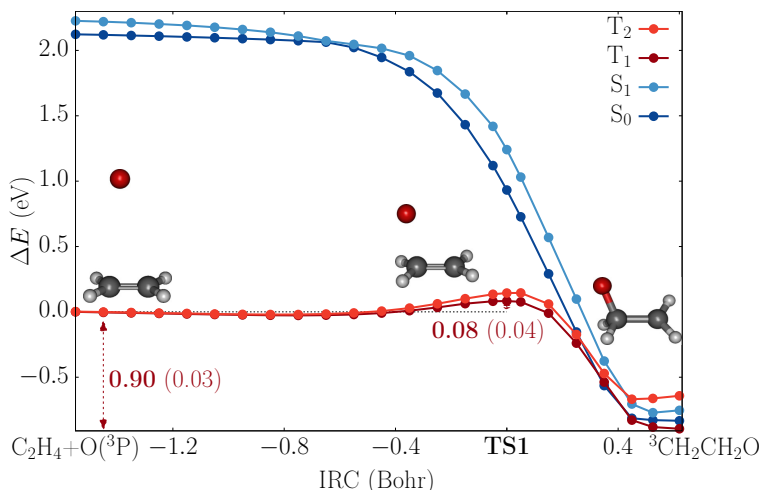


Figure 4: MS2-CASPT2 singlet and triplet potential energy profiles along the IRC related to TS1, between the reactants $O(^3P) + C_2H_4$ and the minimum on the T_1 3CH_2CH_2O . Relative energies are in eV, and values in parentheses are the differences with the values obtained in Ref. [15].

The states T_1 and T_2 show a similar profile, correctly dissociating to the same asymptote, as the system must “evolve” towards the two uncharged fragments $O(^3P) + C_2H_4$: the two unpaired electrons can be distributed into two of the three degenerate oxygen p orbitals, forming the two degenerate states T_1 and T_2 . This observation is confirmed by the spin density analysis, which shows two unpaired electrons localized on the oxygen atom. The pair of states S_0 and S_1 follow approximately the same profile remaining parallel to each other along the IRC coordinate, except between IRC -0.8 and -0.4, where a state crossing takes place. The analysis of the CASSCF configuration reveals that for such singlet states the system heads again towards two neutral fragments: state S_0 is related to $O(^1D)$, while in S_1 is related to $O(^1S)$. The CASSCF energy profiles shown in Figure S5 of the Supporting Information qualitatively agree with the corresponding CASPT2 curves. Overall, it is encouraging that, while the energetics are slightly different, in particular near the transition state TS1 where the energy barrier is overestimated by 0.27 eV with respect to the Ref. [15], the qualitative behavior between CASSCF and CASPT2 is similar. The CCSD(T) calculations shown in Figure S12 and in Figure S13 of the Supporting Information confirm again

the accuracy of the overall CASPT2 calculations, as the CCSD(T) profiles perfectly match the CASPT2 ones for the triplet state T_1 . For singlet states there is a substantial deviation around the minimum ${}^3\text{CH}_2\text{CH}_2\text{O}$, as in this region the system becomes multiconfigurational, as can be seen by the increase of the T1 diagnostic around the biradical region.

- $\text{CH}_2\text{CHO} + \text{H}$ triplet dissociation pathway. *Pathway (1) of the Introduction.*s The energy curves related to the $\text{CH}_2\text{CHO} + \text{H}$ dissociation pathway are shown in Figure 5. This pathway is generated starting from the triplet minimum ${}^3\text{CH}_2\text{CH}_2\text{O}$, leading eventually to the two dissociated fragments through the transition state TS3. The two minima and the transition state optimized in CASSCF are well reproduced by the MS-CASPT2 singlet point calculations, confirming again that CASSCF provides reasonable geometries. The energy barrier of 0.44 eV at TS3 is in very good agreement with the previous theoretical results, however, the energy gap between the two minima results to be 0.18 eV. This value is smaller than the value reported by Fu et al. [15] (0.56 eV).

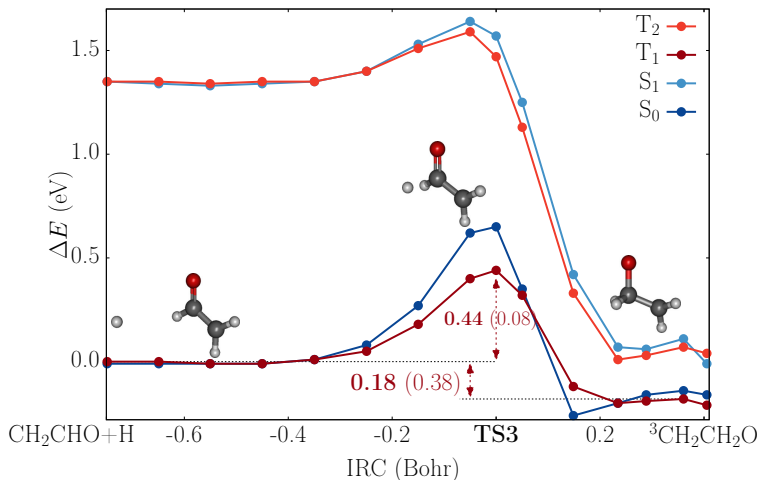


Figure 5: MS2-CASPT2 singlet and triplet potential energy profiles along the IRC related to TS3, between the minimum on the ${}^3\text{CH}_2\text{CH}_2\text{O}$ and the dissociated fragments $\text{CH}_2\text{CHO} + \text{H}$. Relative energies are in eV, and values in parentheses are the differences with the values obtained in Ref. [15].

The analysis of the CASSCF wavefunction on all four states reveals a substantial multiconfigurational character along the entire IRC, as the weights coefficients C^2 are always smaller than 0.90. The spin population analysis for state T_1 and T_2 shows that the system correctly dissociates to two radical fragments¹⁷ $\text{CH}_2\text{CHO}^\bullet$ and H^\bullet . The molecular fragment carries its electron in both oxygen and carbon p orbitals for the T_1 state, and in the oxygen p orbital for the T_2 state, while the H atom has its unpaired electron in the s orbital for both states. The two doublet states of the dissociated fragments can be spin-coupled in a singlet or in a triplet state without changing the asymptotic limit, justifying the similar energy profile and the degeneracy at the asymptotic limit of the pairs S_0/T_1 and S_1/T_2 . Accordingly, singlets and triplets stay very close to each other along the entire IRC, hinting for possible ISCs especially between the states T_1 and S_0 . However, SOC calculations reveal that coupling is noticeable only between the pair of states T_1/S_1 and T_2/S_0 (ranging between 28 and 40 cm^{-1}) which are energetically close only in the triplet minimum region. For the pair S_0/T_1 and S_1/T_2 SOC always remains smaller than 5 cm^{-1} . This observation is particularly relevant because it clearly shows the importance of the molecular geometry in determining the strength of SOC, and even though two electronic states of different spin multiplicity are close in energy, like T_1 and S_0 , a small SOC is likely to prevent ISC. The CASSCF energy profiles are shown in Figure S6 of the Supporting Information and are in good agreement with the CASPT2 results. In this case, the energy gaps between the critical points are consistent in both level of theories. The energy barrier at TS3 is very well reproduced by the CASSCF, as well as the energy difference between the two minima is in agreement with the corresponding CASPT2 value, albeit this energy gap is further reduced to 0.10 eV in CASSCF. Nevertheless, both theories agree on the same mechanistic picture, confirming that the states S_0 , S_1 , and T_2 are likely to be populated near the triplet minimum, where ISC is likely to occur. We performed CCSD(T) calculations on the lowest singlet and triplet states, shown

in Figure S14 and Figure S15 of the Supporting Information. As expected, for this pathway the coupled-cluster energies do not match the corresponding CASSCF and CASPT2 profiles, because of the considerable static electron correlation retained by the system along this IRC coordinate.

- *CH₂ + H₂CO triplet dissociation pathway. Pathway (2) of the Introduction.* This pathway begins at the triplet minimum, and via the transition state TS4 leads to a C-C bond breaking and to the formation of two dissociated fragments CH₂ + H₂CO. The corresponding MS-CASPT2 energy profiles are shown in Figure 6. Similarly to the results shown above, the lowest triplet state T₁ is in very good agreement with earlier studies at the same geometries, as the maximum energy deviation at the critical points is smaller than 0.1 eV. Note also that the CASSCF optimized critical points are once more very well reproduced by the CASPT2 as shown in Figure S7 of the Supporting Information. It is worth noting that for this IRC pathway, the electronic states are well separated in energy at the asymptotic limit, meaning that each state converges to a completely different electronic configuration. Indeed, the analysis of both CASSCF wavefunction and spin population shows that on the T₁ state the system undergoes an etherolitic C-C bond breaking, with the two unpaired electrons localized on the CH₂ fragment, whereas for the T₂ state there is a homolitic C-C bond breaking, with both fragments carrying an unpaired electron. The multiconfigurational character is also very different for both states: T₁ shows a single-references character with only one leading determinant with a weight > 0.90, while T₂ shows a strong multiconfigurational character, as three important doubly-excited determinants contribute to the electronic state, with weights 0.47, 0.31, 0.16.

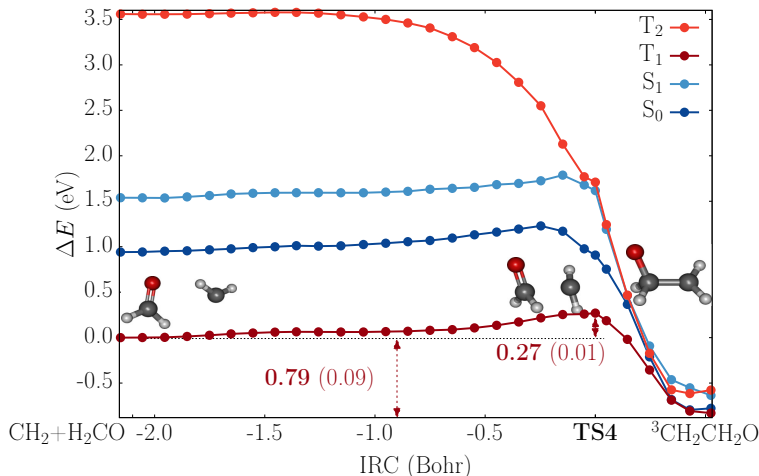


Figure 6: MS2-CASPT2 singlet and triplet potential energy profiles along the IRC related to TS4, between the minimum on the T_1 energy ${}^3\text{CH}_2\text{CH}_2\text{O}$ and the dissociated fragments. Relative energies are in eV, and values in parentheses are the differences with the values obtained in Ref. [15].

For the singlet S_0 , the *closed-shell* configuration is the only important configuration at the asymptotic limit with a weight of 0.86, meaning that this state has a multi-configurational character, although much smaller than T_2 . For S_1 there is only one important configuration that contributes with a weight larger than 0.90. The study of the CASSCF wavefunction reveals that on S_0 the C-C bond breaking is etherolitic, whereas for the state S_1 it is homolitic, similar to the triplet states. The corresponding CASSCF energy profiles shown in Figure S7 of the Supporting Information are in fairly good agreement with CASPT2, although with less accurate relative energies. In both cases, it is clear that the states S_0 , S_1 , T_2 become important only in the region between TS4 and the triplet minimum where all four states are energetically close. The CCSD(T) energy profiles in Figure S16 and in Figure S17 of the Supporting Information show a very good agreement for the triplet T_1 , where CCSD(T) profile perfectly matches the corresponding CASPT2. For the singlet state S_0 the agreement between the coupled-cluster and the CASPT2 is considerably worse than for the triplet state, in agreement with the important nondynamic correlation at the asymptotic limit as well as near the triplet minimum. For such state, single-references methods are not

reliable.

- *CH₃ + CHO singlet dissociation pathway. Last part of pathway (3) of the Introduction.*

This dissociation pathway begins at the singlet minimum CH₃CHO, which leads to the two fragments CH₃+CHO via a to C-C bond breaking. The MS-CASPT2 energy profiles related to this pathway are shown in Figure 7. In this case, the asymptotic limit is reached via a LITP, i.e. interpolating between the CH₃CHO singlet minimum and the two fragments CH₃ + CHO obtained via a C-C bond stretching up to 5.0 Å. The S₀ profile shows no sign of a transition state, as the energy increases monotonically towards the asymptotic region, in agreement with previous calculations by Fu et al. [15]. The dissociation energy of 4.23 eV results to be overestimated by 0.3 eV with respect to previous calculations.¹⁵ However, this overestimation is expected to some extent, as the two separated fragments CH₃ and CHO have not been optimized. The singlet excited state S₁ shows a behaviour similar to the S₀, with the energy increasing monotonically towards the asymptotic region. The corresponding SA-CASSCF singlet energy profiles shown in Figure S8 of the Supporting Information show a smooth behavior, similar to the MS-CASPT2 profiles, proving once again that the chosen computational protocol and related active space are reliable for the study reported in this work. The analysis of the CASSCF wavefunction reveals non-negligible multiconfigurational character for both singlet states ($C^2 \sim 0.88$) in the region close to the minimum CH₃CHO, upon the C-C bond stretching/breaking, whereas near the two fragments CH₃ and CHO the system acquires a single reference character. In fact, in the asymptotic region, no other chemical rearrangements are obtained. The MS-CASPT2 triplet states T₁ and T₂ in Figure 7 show a peak near the minimum CH₃CHO. The shape of the potential energy curves suggests the appearance of an avoided crossings near CH₃CHO. Indeed, a detailed analysis of the triplet CASSCF configurations along the LITP revealed that a higher state (T₃, not shown in Figure 7) rapidly decreases in energy along the LITP, following the character of T₂ and then of T₁ after the avoided crossings; the lowest

triplet state, T_1 , in turn, increases in energy towards CH_3CHO , following the T_2 character, and eventually then following the T_3 character. In this region both states show a strong multiconfigurational character, whereas in the asymptotic region the system becomes single reference. Towards the asymptotic region T_1 becomes degenerate with S_0 , and T_2 becomes degenerate with S_1 , for the same reasons already discussed for pathway (1). The triplet state crossing discussed above affects the stability of the active space solution, which undergoes a large orbital rotation for one doubly occupied orbital towards an orbital outside the active space. Nevertheless, such instability does not concern the singlet states, for which this pathway has been investigated, meaning the computational procedure is still reliable. Furthermore, note that, according to previous calculations, the triplet states should not be populated when the system undertakes this dissociation channel.

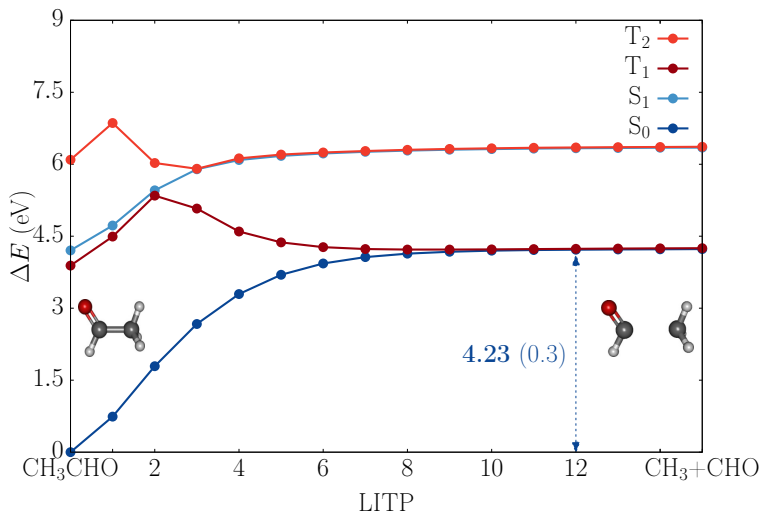


Figure 7: MS2-CASPT2 singlet and triplet potential energy profiles along the LITP between the minimum on the S_0 energy CH_3CHO and the dissociated fragments CH_3+CHO . Relative energies are in eV, and values in parentheses are the differences with the values obtained in Ref. [15].

- *$\text{CH}_3\text{CO} + \text{H}$ singlet dissociation pathway. Last part of pathway (4) of the Introduction.*
This pathway begins at the singlet minimum CH_3CHO as for pathway (3), but in this case the two fragments $\text{CH}_3\text{CO} + \text{H}$ are produced by a C-H bond breaking. Therefore,

the procedure employed to analyze this pathway is similar to the previous point, where LITP is used to generate the intermediate geometries between CH_3CHO and the two fragments by a simple C-H rigid bond elongation up to 5.0 \AA . The MS-CASPT2 energy profiles related to this pathway are shown in Figure 8. The overall evolution of the four states is very similar to pathway (3) presented above. The singlet states show a smooth monotonic profile with no sign of transition states, in agreement with previous calculations.¹⁵ The S_0 dissociation energy barrier of 3.75 eV is in this case underestimated by CASPT2 of about 0.39 eV . The corresponding CASSCF singlet energy profiles shown in Figure S9 of the Supporting Information appear very smooth as well, and qualitatively similar to the CASPT2 profiles. It is worth pointing out the smooth changes of the active space starting with the set of orbitals shown in Figure 2. In particular, Figure S1 of the Supporting Information shows the transformation of the $3p_x$ orbital, which smoothly rotates towards a σ_{CH}^* , an orbital of utmost importance for an accurate description of the electronic structure of the system during the C-H bond breaking. The analysis of the multiconfigurational character of the electronic states reveals strong similarities with pathway (3).

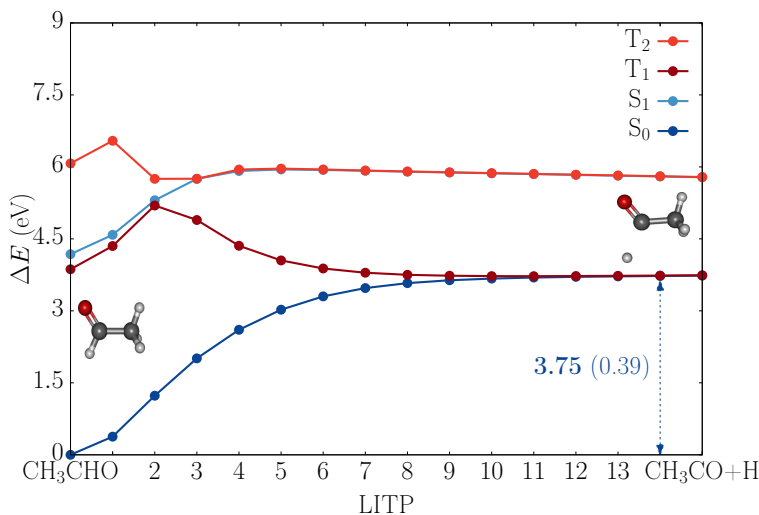


Figure 8: MS2-CASPT2 singlet and triplet potential energy profiles along the LITP between the minimum on the S_0 energy CH_3CHO and the dissociated fragments $\text{CH}_3\text{CO}+\text{H}$. Relative energies are in eV, and values in parentheses are the differences with the values obtained in Ref. [15].

- *CH₂CO + H₂ singlet dissociation pathway. Last part of pathway (5) of the Introduction.*

This pathway involves two C-H bond breaking and one H-H bond formation, leading to the products CH₂CO + H₂. In this case, the active space results to be unstable for both multiplicities, as one active orbital undergoes a large rotation during the first C-H bond stretching of the CH₃ group. According to previous work,¹⁵ this pathway involves a transition state called TS6. We determined such intermediate configuration using DFT (results not shown), since CASSCF optimization results to be inaccurate due to the active space instability. Generating an IRC path based on DFT geometries, and performing single point energy calculations at the CASSCF level with the active space of Figure 2, we find for both multiplicities participation of a higher energy state which eventually becomes the lowest state, S₀ and T₁. The large orbital rotation is most likely caused by this rapid state crossing which introduces important rearrangements of the electronic structure. In order to overcome this limitation, a larger active space should be used, together with a SA-CASSCF calculation including higher energy states. However, we believe that due to the low probability of this reaction channel (< 4% according to previous surface-hopping calculations¹⁹) and to the increase of the computational cost, which would prevent us from extending this procedure to the pathways previously analyzed, further investigation of pathway (5) is beyond the scope of our study.

4 Conclusions

We reported accurate multiconfigurational calculations for the lowest two singlet and two triplet states S₀, S₁, T₁, T₂, along the most probable reaction pathways in the O(³P)+C₂H₄ reaction. These calculations confirmed previous interpretations based on surface hopping,¹⁵ providing at the same time further insights into the multiconfigurational character of the system, pointing out the regions where and the reasons why the nondynamical correlation

becomes important. By choosing an adequate CASSCF active space, we were able to perform CASSCF/CASPT2 calculations, providing a detailed analysis of the electronic structure of the system and the topology of the states involved in the scattering reaction. Furthermore, we enriched information from the previous studies on this system by assessing the performance of various ab-initio methods such as CASSCF, CASPT2 and CCSD(T) along the most important reactive pathways. Such assessment makes this work very useful in the perspective of on-the-fly dynamics simulations, and at the same time disentangles the complex electronic structure information from the results of the dynamics simulations.

Our new calculations uncover that the system becomes highly multiconfigurational near the triplet minimum ${}^3\text{CH}_2\text{CH}_2\text{O}$ and the singlet transition state TS0, especially for the singlet states S_0 and S_1 , whereas for the triplet states the system shows most of the time a single-reference character. Such multiconfigurational character is found also in certain dissociation channels at the asymptotic limit. In these particular regions where nondynamic correlation becomes important, single-reference methods such as DFT or CCSD(T) fail to describe the properties of the singlet states, although they would be able to recover most of the electronic properties of the triplet states. Such theoretical methods are thus not suitable for on-the-fly calculations. The CASPT2 method describes very well the electronic properties and the topology of both multiplicities, which would make it suitable for on-the-fly calculations. However, its computational cost is high, that is why we oriented the analysis towards the assessment of the CASSCF results. CASSCF recovers most of the electronic properties of the four states, as the potential energy profiles are qualitatively in agreement with the corresponding CASPT2 ones, although the energies are not as accurate as in CASPT2. In order to employ CASSCF in future dynamical on-the-fly studies of the reaction $\text{O}({}^3\text{P})+\text{C}_2\text{H}_4$, the energy differences with respect to CASPT2 needs to be taken care of. Developments in this direction are currently ongoing.

An additional feature of the $\text{O}({}^3\text{P})+\text{C}_2\text{H}_4$ collision reaction that our work highlights is the presence of a degeneracy region between the analyzed singlet states, namely the conical

intersection between S_0 and S_1 . The conical intersection appears at a molecular geometry that is very close to the TS0 geometry, and is energetically accessible. Therefore, in this region, both IC and ISC might occur, being mediated by the conical intersection and by SOC, respectively. This observation calls for an assessment of the reaction dynamics including all four states analyzed in this work. In fact, while it is not straightforward to precisely assess the competing effects on the dynamics of IC and ISC near the TS0 geometry, one could expect that a transition from T_1 to S_0 is accompanied by a transition towards S_1 at (or in the vicinity) of the degeneracy point. If this happens, the molecule might re-enter the lowest singlet state with some delay or in a slightly different configuration, if compared to the case where only S_0 and T_1 are considered. In order to shed some light on these effects, comparative dynamical studies including two electronic state and four electronic state might reveal highly informative.

Acknowledgement

The authors thank Carine Clavaguéra for insightful discussions. This work is supported by a public grant from the “Laboratoire d’Excellence Physics Atoms Light Mater” (LabEx PALM) overseen by the French National Research Agency (ANR) as part of the “Investissements d’Avenir” program (reference: ANR-10-LABX-0039-PALM).

Supporting Information

Supporting information is available, which contains:

- Cartesian coordinates (in Å) as xyz files of the critical geometries optimized at the CASSCF level for: CH_2OCH_2 , CH_3CHO , TS0, CI(S_0 - S_1), $^3\text{CH}_2\text{CH}_2\text{O}$, TS1, TS3, TS4, $\text{O}(^3\text{P})+\text{C}_2\text{H}_4$, $\text{CH}_2\text{CHO}+\text{H}$, $\text{CH}_2+\text{H}_2\text{CO}$.
- Tables and figures reporting details about energies (at CASPT2, CASSCF and CCSD(T))

levels) along IRC and LITP as well as about the active space.

References

- (1) Gardiner, W. C. *Gas-Phase Combustion Chemistry*; Springer-Verlag, 2000.
- (2) Wayne, R. P. *Chemistry of Atmospheres*; Oxford University Press: Oxford, U.K., 2000.
- (3) Hu, W.; Lendvay, G.; Maiti, B.; Schatz, G. C. Trajectory Surface Hopping Study of the O(3P) + Ethylene Reaction Dynamics. *J. Phys. Chem. A* **2008**, *112*, 2093–2103, PMID: 18088105.
- (4) Banks, B. A.; deGroh, K. K.; Miller, S. K. Low Earth Orbital Atomic Oxygen Interactions With Spacecraft Materials. *NASA/TM* **2004**,
- (5) Banks, B. A.; Backus, J. A.; Manno, M. V.; Waters, D. L.; Cameron, K. C.; deGroh, K. K. Atomic oxygen erosion yield prediction for spacecraft polymers in low earth orbit. *NASA/TM* **2009**,
- (6) Casavecchia, P.; Leonori, F.; Balucani, N. Reaction dynamics of oxygen atoms with unsaturated hydrocarbons from crossed molecular beam studies: primary products, branching ratios and role of intersystem crossing. *Int. Rev. Phys. Chem.* **2015**, *34*, 161–204.
- (7) Occhiogrosso, A.; Viti, S.; Balucani, N. An improved chemical scheme for the reactions of atomic oxygen and simple unsaturated hydrocarbons - implications for star-forming regions. *Monthly Notices of the Royal Astronomical Society* **2013**, *432*, 3423–3430.
- (8) Belbruno, J. J. Ab initio calculations of the potential energy surfaces for the unimolecular dissociation reaction of ethylene oxide. *J. Phys. Org. Chem.* **1997**, *10*, 113–120.

- (9) Shepler, B. C.; Braams, B. J.; Bowman, J. M. Quasiclassical Trajectory Calculations of Acetaldehyde Dissociation on a Global Potential Energy Surface Indicate Significant Non-transition State Dynamics. *J. Phys. Chem. A* **2007**, *111*, 8282–8285, PMID: 17676724.
- (10) Kurosaki, Y. Hydrogen-atom production channels of acetaldehyde photodissociation: Direct DFT molecular dynamics study. *J. Mol. Struct.: THEOCHEM* **2008**, *850*, 9 – 16.
- (11) Shepler, B. C.; Braams, B. J.; Bowman, J. M. Roaming. Dynamics in CH₃CHO Photodissociation Revealed on a Global Potential Energy Surface. *J. Phys. Chem. A* **2008**, *112*, 9344–9351, PMID: 18597443.
- (12) Tapavicza, E.; Tavernelli, I.; Rothlisberger, U.; Filippi, C.; Casida, M. E. Mixed time-dependent density-functional theory/classical trajectory surface hopping study of oxirane photochemistry. *J. Chem. Phys.* **2008**, *129*, 124108.
- (13) Han, Y.-C.; Shepler, B. C.; Bowman, J. M. Quasiclassical Trajectory Calculations of the Dissociation Dynamics of CH₃CHO at High Energy Yield Many Products. *J. Phys. Chem. Lett.* **2011**, *2*, 1715–1719.
- (14) Fu, B.; Han, Y.-C.; Bowman, J. M.; Angelucci, L.; Balucani, N.; Leonori, F.; Casavecchia, P. Intersystem crossing and dynamics in O(³P)+C₂H₄ multichannel reaction: Experiment validates theory. *Proc. Natl. Acad. Sci. U.S.A* **2012**, *109*, 9733–9738.
- (15) Fu, B.; Han, Y.-C.; Bowman, J. M.; Leonori, F.; Balucani, N.; Angelucci, L.; Occhiogrosso, A.; Petrucci, R.; Casavecchia, P. Experimental and theoretical studies of the O(³P) + C₂H₄ reaction dynamics: Collision energy dependence of branching ratios and extent of intersystem crossing. *J. Chem. Phys.* **2012**, *137*, 22A532.
- (16) Balucani, N.; Leonori, F.; Casavecchia, P.; Fu, B.; Bowman, J. M. Crossed Molecular Beams and Quasiclassical Trajectory Surface Hopping Studies of the Multichannel

- Nonadiabatic O(³P) + Ethylene Reaction at High Collision Energy. *J. Phys. Chem. A* **2015**, *119*, 12498–12511, PMID: 26413909.
- (17) Li, X.; Jasper, A. W.; Zádor, J.; Miller, J. A.; Klippenstein, S. J. Theoretical kinetics of O + C₂H₄. *Proc. Combust. Inst* **2017**, *36*, 219 – 227.
- (18) Curchod, B. F. E.; Agostini, F.; Tavernelli, I. CT-MQC - a coupled-trajectory mixed quantum/classical method including nonadiabatic quantum coherence effects. *Eur. Phys. J. B* **2018**, *91*.
- (19) Fu, B.; Han, Y.-C.; Bowman, J. M.; Leonori, F.; Balucani, N.; Angelucci, L.; Occhiogrosso, A.; Petrucci, R.; Casavecchia, P. Experimental and theoretical studies of the O(³P) + C₂H₄ reaction dynamics: Collision energy dependence of branching ratios and extent of intersystem crossing. *J. Chem. Phys.* **2012**, *137*, 22A532.
- (20) Min, S. K.; Agostini, F.; Tavernelli, I.; Gross, E. K. U. Ab Initio Nonadiabatic Dynamics with Coupled Trajectories: A Rigorous Approach to Quantum (De)Coherence. *J. Phys. Chem. Lett.* **2017**, *8*, 3048–3055.
- (21) Agostini, F.; Curchod, B. F. E.; Vuilleumier, R.; Tavernelli, I.; Gross, E. K. U. In *Handbook of Materials Modeling : Methods: Theory and Modeling*; Andreoni, W., Yip, S., Eds.; Springer International Publishing: Cham, 2018; pp 1–47.
- (22) Agostini, F.; Gross, E. K. U. In *Quantum Chemistry and Dynamics of Excited States: Methods and applications*; Andreoni, W., Yip, S., Eds.; 2020.
- (23) Cavallotti, C.; Leonori, F.; Balucani, N.; Nevrlý, V.; Bergeat, A.; Falcinelli, S.; Vanuzzo, G.; Casavecchia, P. Relevance of the Channel Leading to formaldehyde + triplet ethylidene in the O(³P) + propene reaction under combustion conditions. *J. Phys. Chem. Lett.* **2014**, *5*, 4213–4218.

- (24) Leonori, F.; Balucani, N.; Nevrlý, V.; Bergeat, A.; Falcinelli, S.; Vanuzzo, G.; Casavecchia, P.; Cavallotti, C. Experimental and theoretical studies on the dynamics of the $O(^3P) + \text{propene}$ reaction: Primary products, branching ratios, and role of intersystem crossing. *J. Phys. Chem. C* **2015**, *119*, 14632–14652.
- (25) Gonzalez-Lavado, E.; Corchado, J. C.; Suleimanov, Y. V.; Green, W. H.; Espinosa-Garcia, J. Theoretical Kinetics Study of the $O(^3P) + \text{CH}_4/\text{CD}_4$ Hydrogen Abstraction Reaction: The Role of Anharmonicity, Recrossing Effects, and Quantum Mechanical Tunneling. *J. Phys. Chem. A* **2014**, *118*, 3243–3252.
- (26) Mellouki, A.; Wallington, T. J.; Chen, J. Atmospheric chemistry of oxygenated volatile organic compounds: Impacts on air quality and climate. *Chem. Rev.* **2015**, *115*, 3984–4014.
- (27) Ibele, L. M.; Curchod, B. F. E. A molecular perspective on Tully models for nonadiabatic dynamics. *Phys. Chem. Chem. Phys.* **2020**, *22*, 15183–15196.
- (28) Finley, J.; Malmqvist, P.-Å.; Roos, B. O.; Serrano-Andrés, L. The multi-state CASPT2 method. *Chem. Phys. Lett.* **1998**, *288*, 299.
- (29) Ghigo, G.; Roos, B. O.; Malmqvist, P.-Å. A modified definition of the zeroth-order Hamiltonian in multiconfigurational perturbation theory (CASPT2). *Chem. Phys. Lett.* **2004**, *396*, 142.
- (30) Zobel, J. P.; Nogueira, J. J.; González, L. The IPEA dilemma in CASPT2. *Chem. Sci.* **2017**, *8*, 1482.
- (31) Widmark, P.-O.; Malmqvist, P.-Å.; Roos, B. O. Density matrix averaged atomic natural orbital (ANO) basis sets for correlated molecular wave functions. II. Second row atoms. *Theor. Chim. Acta* **1991**, *79*, 419–432.

- (32) Widmark, P.-O.; Malmqvist, P.-Å.; Roos, B. O. Density matrix averaged atomic natural orbital (ANO) basis sets for correlated molecular wave functions. I. First row atoms. *Theor. Chim. Acta* **1990**, *77*, 291–306.
- (33) Galván, I. F.; Vacher, M.; Alavi, A.; Angeli, C.; Aquilante, F.; Autschbach, J.; Bao, J. J.; Bokarev, S. I.; Bogdanov, N. A.; Carlson, R. K.; et al. OpenMolcas: From Source Code to Insight. *J. Chem. Theory Comput.* **2019**, *15*, 5925–5964.
- (34) Doehnert, D.; Koutecky, J. Occupation numbers of natural orbitals as a criterion for biradical character. Different kinds of biradicals. *J. Am. Chem. Soc.* **1980**, *102*, 1789–1796.
- (35) Kubo, T.; Shimizu, A.; Sakamoto, M.; Uruichi, M.; Yakushi, K.; Nakano, M.; Shioimi, D.; Sato, K.; Takui, T.; Morita, Y.; et al. Synthesis, Intermolecular Interaction, and Semiconductive Behavior of a Delocalized Singlet Biradical Hydrocarbon. *Angew. Chem. Int. Ed.* **2005**, *44*, 6564–6568.
- (36) Malmqvist, P. Å.; Roos, B. O.; Schimmelpfennig, B. The restricted active space (RAS) state interaction approach with spin-orbit coupling. *Chem. Phys. Lett.* **2002**, *357*, 230–240.
- (37) Purvis, G. D.; Bartlett, R. J. A full coupled-cluster singles and doubles model: The inclusion of disconnected triples. *J. Chem. Phys.* **1982**, *76*, 1910–1918.
- (38) Pople, J. A.; Head-Gordon, M.; Raghavachari, K. Quadratic configuration interaction. A general technique for determining electron correlation energies. *J. Chem. Phys.* **1987**, *87*, 5968–5975.
- (39) Neese, F. The ORCA program system. *WIREs Comput. Mol. Sci.* **2012**, *2*, 73–78.
- (40) Neese, F. Software update: the ORCA program system, version 4.0. *WIREs Comput. Mol. Sci.* **2018**, *8*, e1327.

- (41) Woon, D. E.; Dunning, T. H. Gaussian basis sets for use in correlated molecular calculations. III. The atoms aluminum through argon. *J. Chem. Phys.* **1993**, *98*, 1358–1371.
- (42) Fleming, G.; Anderson, M. M.; Harrison, A. J.; Pickett, L. W. Effect of Ring Size on the Far Ultraviolet Absorption and Photolysis of Cyclic Ethers. *J. Chem. Phys.* **1959**, *30*, 351–354.
- (43) Hadad, C. M.; Foresman, J. B.; Wiberg, K. B. Excited states of carbonyl compounds. 1. Formaldehyde and acetaldehyde. *J. Phys. Chem.* **1993**, *97*, 4293–4312.
- (44) Krenz, M.; Gerstmann, U.; Schmidt, W. G. Photochemical Ring Opening of Oxirane Modeled by Constrained Density Functional Theory. *ACS Omega* **2020**, *5*, 24057–24063.
- (45) Gomer, R.; Noyes, W. A. Photochemical Studies. XLII. Ethylene Oxide. *J. Am. Chem. Soc.* **1950**, *72*, 101–108.
- (46) Kawasaki, M.; Ibuki, T.; Iwasaki, M.; Takezaki, Y. Vacuum-ultraviolet photolysis of ethylene oxide. *J. Chem. Phys.* **1973**, *59*, 2076–2082.
- (47) El-Sayed, M. A. Spin-Orbit Coupling and the Radiationless Processes in Nitrogen Heterocyclics. *J. Chem. Phys.* **1963**, *38*, 2834–2838.
- (48) Ess, D. H.; Johnson, E. R.; Hu, X.; Yang, W. Singlet-Triplet Energy Gaps for Diradicals from Fractional-Spin Density-Functional Theory. *J. Phys. Chem. A* **2011**, *115*, 76–83.
- (49) Lee, T.; Rice, J.; Scuseria, G.; Schaefer, H. F. Theoretical investigations of molecules composed only of fluorine, oxygen and nitrogen: determination of the equilibrium structures of FOOF, (NO)₂ and FNNF and the transition state structure for FNNF cis-trans isomerization. *Theoret. Chim. Acta* **1989**, *75*, 81.
- (50) Lee, T. J.; Taylor, P. R. A diagnostic for determining the quality of single-reference electron correlation methods. *Int. J. Quantum Chem.* **1989**, *36*, 199–207.

Graphical TOC Entry

